Performance Assessment of Relay-based Network Coding in the Smart Grid Networks

Nikos I. Passas

Department of Informatics and Telecommunications, University of Athens, Athens, Greece

Abstract In this paper we present an experimental testbed and performance evaluation results that have been specifically been set up to measure the potential of employing a simplified network coding protocol that is based on the use of bitwise XOR in an intermediate relay node. The research presented in this paper aim to reveal the potential benefits of using network coding in Smart Grid environments in terms of bit error rate improvement at the utility.

Keywords Smart Grid, experimental assessment, bit error rate, network coding

Introduction

The nowadays power grid deployed and used in every country worldwide has served relatively well in providing a seamless unidirectional power supply of electricity. Nevertheless, today a new set of challenges is arising it is currently facing new challenges, such as the depletion of primary energy resources, the diversification of energy generation, and the climate change [1]. Furthermore, conventional power grids lack the capability of (real-time) monitoring and controlling the various appliances to provide optimal full system-wide energy usage. Therefore, the existing power grid is evolving into a more intelligent, more responsive, more efficient, and more environmentally friendly system, known as the Smart Grid (SG) [2]. To fully exploit the power of such new SG paradigm, efficient, reliable and secure two-way information flow among the customers and the utility companies is mandatory. In this perspective, the smart meters are new devices with the necessary intelligence to enable that two-way communication, since they are capable of collecting and delivering punctual power consumption information to remote utilities much more efficiently than conventional meters [3]. By using this information, utility companies are able to better monitor the energy consumption and to adapt the generation of energy accordingly.

Utility companies are then able to setup Smart Energy Networks (SENs) to better monitor the energy consumption and to advice on changes of users' behavior, using proper smart energy algorithms [4]. The smart meter collects the power consumption information of the dishwasher, TV, and the refrigerator, and also sends the control commands to them, if necessary. The data generated by the smart meters in different buildings is transmitted to a data aggregator. This aggregator could be an access point or gateway. This data can be routed to the electric utility or the distribution substation.

At present, much effort is being made by the utility companies to install these smart meters into millions of homes across Europe. European regulations require member nations to ensure that 80% of residential households are fitted with a smart meter by 2020 [5]. With the help of these densely deployed smart meters, SENs offer numerous benefits for consumers, operators, and the community as a whole.

As for the consumers, SENs will help moderating their energy usage to reduce waste, lower their monthly bill, and use power in a more sustainable way. As for the operators/industry, SENs will help preventing outages, shorten the response time to problems, reduce cost and increase efficiency, and allow operators to resolve issues remotely. It will also integrate renewable energy and reduce carbon emissions on a macro and micro level. As

for the community as a whole, SENs will help creating a safer, more secure, more reliable grid, and will reduce dependency on foreign energy supplies. This will reduce carbon emissions and will combat global warming.

Communications are one of the main pillars for the realization of the Smart Grid. With the integration of advanced technologies and applications for implementing a smarter electricity grid, a huge amount of data from different applications will be generated for further analysis, control and real-time pricing. To this end, the identification of the best communication technologies that enable efficient handling of the output data and the delivery of a reliable, secure and cost-effective service throughout the SG system is critical for the utility operators [6]. The outage management after disasters in the future power grid, will strongly depend on the smooth interplay between the electricity grid and all communications systems involved through its maintenance and operation.

The transmission of data between the smart meters and the utility companies can be transferred over both wired and wireless communication technologies. The key advantage of the former technologies relies on their low deployment cost and easy installation in remote areas in an ad hoc fashion. Such features enable the efficient transfer of data between the sensor/measurement nodes in the Home Area Network (HAN) and the Neighbor Area Network (NAN) as well as the advanced metering infrastructure (AMI) in a network-wide scale. Nevertheless, wireless communication technologies are more vulnerable to small scale fading and path loss. In the contrary, wired communication technologies are typically interference-free and do not require the utilization of batteries at the sensor nodes. These two features highlight their capacity to better support broadband connectivity between the smart meter infrastructure and the utility companies as compared to their wireless competitors.

From the above discussion, it becomes apparent that both the wireless and the wired communication technologies feature different limiting factors and meet heterogeneous performance requirements. Hence, the adoption of a specific networking technology for communications in the Smart grid should account such limiting factors, and fine-tuned based on the specific environment under scope with respect to parameters that include the time of deployment, the operational costs, as well as the availability of the technology in rural/urban or indoor/outdoor environments. Besides, among others, efficient and reliable networking that specifically aims to enable two-way communications between the smart meters and the utility companies and ensure that the power control centers are timely informed of the energy consumption throughout the electricity grid is critical.

Today the classical store-and-forward paradigm is used in most networks. With store-and-forward packet sent from a receiver traverses nodes in a network unchanged until it reach the intended destination. Thus, the nodes in the network do not modify the data in the transmitted packet, hence the name store-and-forward. Ahlswede et. al. [7] demonstrated that in some topologies the max-flow min-cut bound [8] cannot be obtained by existing routing protocols that are based on the premise of store-and-forward. To solve this problem they proposed network coding (NC) which breaks with this paradigm by enabling nodes in the network in between the source and the destination to modify packets in order to make them more suitable for transmission. In this sense, the first major feature of NC compared against traditional coding and routing techniques is that information itself is treated as algebraic entity on which network nodes are able to operate. Hence, NC follows the compute-and-forward paradigm providing new ways to increase throughput, reliability, performance, security, error correction and operation.

Consequently NC-based schemes have been proposed for a wide range of networks and applications. In cellular networks [9] it has been proposed as the means to improve throughput and extend coverage, reduce network deployment costs. Noticeably, it is often used in combination with relaying techniques. In wireless meshed networks [10], it has been demonstrated to improve robustness, throughput and reduce the complexity of self-organization [11-12].

To the remainder of this paper, we provide an experimental assessment of the bit error rate improvement offered Relay-based NC in smart grid environments. The simplified bitwise XO feedback that is provided by an intermediate relay node to the final destination of the packets as an additional error control and correction input. The remainder of this paper is organized as follows. In section II, we overview our experimental testbed setup for assessing the performance of the simplified NC protocol mentioned above, detailing the equipment used and the roles of the intermediate architecture entities. In section III, we present the NC protocol under scope. In

section IV we include our experimental evaluation results and discussions on the potential benefits following from the employment of the proposed NC protocol. Finally, section V concludes this paper providing valuable insights for future work and research in the area.

Experimental testbed setup

A schematic diagram of the experimental smart grid testbed is provided in Fig. 1. In the sequel, we briefly highlight the main operation and role of the entities of the assumed architecture, including information on the utilized equipment (*i.e.* specification, platforms and so on).

The **central unit (CU)** plays the role of a local electricity operator with advanced energy management capabilities and implements a two-threshold energy management protocol which, in the presence of partial power outages, can control the operation of the end devices connected at the bottom part of Fig. 1 in the energy meters. In brief, when the energy consumption is within the range of the support that can be provided by the system, the CU sets up the aggregator unit to send only measurements reports for the aggregated energy consumption. However, when offered load is higher than the one that can be supported, the CU requires for detailed energy consumption per smart meter and decides on how the offered loads of the end devices should be planned and rescheduled. The CU is implemented using a standard desktop PC.
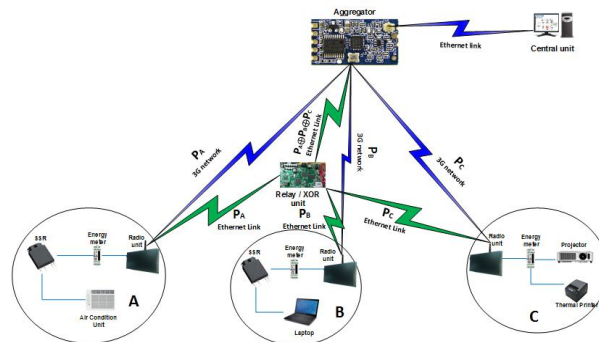

Figure 1: Schematic diagram of the testbed

Table 1: Technical Overview of the equipment used for the AG and the Radio Units

Orytel Skylog 4 Modbus	
General specifications	**Firmware specifications Data acquisition:** Time rated and event triggered(digital I/O changes, analogue input alarms).
Operating voltage: 6V-35V DC. **Current consumption:** 20mA in idle mode, 150 mA in communication GSM 900 (@12V DC) or 100mA in GSM 1800/1900 (@12V DC). **Digital inputs:** 2, opto-isolated switch closures, one towards GND and other towards power supply (ON-OFF).	**Communication modes:** GSM SMS, GSM data or voice calls, GPRS UDP packets.
	Internet communication protocols: IPv4, ICMP, UDP.
Digital outputs: 1 internal relay (contact rate 1A/50V) with one pin internally connected to GND, contacts closed when idle or no power.	**Data communication:** • GSM Data calls asynchronous up to 14,400 bits/s
Serial ports: 1 RS485 supporting Modbus protocol.	• SMS messages (multiple fragmented SMS messages supported)
Temperature range: -10°C, +55°C operating.	• GPRS UDP packets (maximum packet size 900 bytes unfragmented)
Dimensions: 120 x 53 x 30 mm plastic ABS case.	**Alarms:** SMS messages, UDP packets or voice calls to up to two presetable phone numbers. Also activation or deactivation of the digital output.
Protection rating: IP55	**Unit parameters:** All unit parameters can be set/read by means of SMS messages or via host originated data calls or UDP packets.
GSM/GPRS Features	**Interfaces GSM:** SMA jack antenna connector.
Simcom Quad band GSM 850/900/1800/1900 MHz GPRS Class 10. **Output power:** Class 4 (2W at 850/900 MHz) Class 1 (1W at 1800/1900 MHz). **Antenna:** SMA female for external GSM antennas.	**Power and I/O connector:** wire harness 1m long.
	SIM holder: internal 3V SIM cards
	LED indicators: one for GSM/GPRS status and one for modbus status.
	Ethernet: 5 ports of 10/100/1000 Ethernet

The **aggregator unit (AG)** is responsible for collecting the individual energy measurements reported from the three energy meters (smart meters) of the testbed and reporting them periodically to the central unit. The AG unit implements a simplified network coding protocol according to which, apart from collecting the individual measurement reports from the three energy meters shown in Fig. 1, it receives an additional packet from the relay/XOR unit which contains a bitwise XOR version of all three reports from the energy meters. This packet enables the aggregator to identify potential errors in any of the three individual links between the energy meters and the aggregator unit, by comparing the XOR-ed result of the three individual measurements (relay packet) with the individual reports. The AG unit is implemented using an Orytel SKYLOG 4 Modbus remote telemetry unit that is enhanced with the NC protocol capabilities (see Table 1 for some overview of its main technical features).

Figure 2: XOR unit/relay

The **relay/XOR unit (RL)** implements the proposed relay-based NC protocol, which performs bitwise XOR operation over the packets received from the energy meters A, B, and C, and forwards the respective result through a dedicated link to the Aggregator (Ethernet in the testbed). The unit's software is located on non-volatile flash rom which is embedded on the micro controller. The micro controller used is the ATmega2561 with the characteristics shown in Table 2. The unit carries out the required processes and saves the result in the onboard memory. The memory used is the Cypress 62128 with the characteristics shown in Table 3. Finally, the XOR unit is equipped with a Wiznet W5500 card for communication via Ethernet (Table 4 includes technical info).

Table 2: Technical Overview of the micro-controller used for the Relay/XOR unit

ATmega2561
• High Performance, Low Power Atmel® AVR® 8-Bit Microcontroller
• High Endurance Non-volatile Memory Segments – 64K/128K/256KBytes of In-System Self-Programmable Flash – 4Kbytes EEPROM – 8Kbytes Internal SRAM – Write/Erase Cycles:10,000 Flash/100,000 EEPROM – Data retention: 20 years at 85□C/ 100 years at 25□C – Optional Boot Code Section with Independent Lock Bits
• Endurance: Up to 64Kbytes Optional External Memory Space • Atmel® QTouch® library support – Capacitive touch buttons, sliders and wheels – QTouch and QMatrix acquisition – Up to 64 sense channels
• Special Microcontroller Features – Power-on Reset and Programmable Brown-out Detection – Internal Calibrated Oscillator – External and Internal Interrupt Sources – Six Sleep Modes: Idle, ADC Noise Reduction, Power-save, Power-down, Standby,

and Extended Standby
• I/O and Packages
– 54/86 Programmable I/O Lines (ATmega1281/2561,
ATmega640/1280/2560)
– 64-pad QFN/MLF, 64-lead TQFP (ATmega1281/2561)
– 100-lead TQFP, 100-ball CBGA
(ATmega640/1280/2560)
– RoHS/Fully Green

• Temperature Range:
– -40☐C to 85☐C Industrial
• Ultra-Low Power Consumption
– Active Mode: 1MHz, 1.8V: 500µA
– Power-down Mode: 0.1µA at 1.8V

• In-System Programming by On-chip Boot Program

• Advanced RISC Architecture
– 135 Powerful Instructions – Most Single Clock Cycle
Execution
– 32×8 General Purpose Working Registers
– Fully Static Operation
– Up to 16 MIPS Throughput at 16MHz
– On-Chip 2-cycle Multiplier

• Peripheral Features
– Two 8-bit Timer/Counters with Separate Prescaler and
Compare Mode
– Four 16-bit Timer/Counter with Separate Prescaler,
Compare- and Capture Mode
– Real Time Counter with Separate Oscillator
– Four 8-bit PWM Channels
– Six/Twelve PWM Channels with Programmable
Resolution from 2 to 16 Bits
(ATmega1281/2561, ATmega640/1280/2560)
– Output Compare Modulator
– 8/16-channel, 10-bit ADC (ATmega1281/2561,
ATmega640/1280/2560)
– Two/Four Programmable Serial USART
(ATmega1281/2561, ATmega640/1280/2560)
– Master/Slave SPI Serial Interface
– Byte Oriented 2-wire Serial Interface
– Programmable Watchdog Timer with Separate On-chip
Oscillator
– On-chip Analog Comparator
– Interrupt and Wake-up on Pin Change

• Speed Grade:
– ATmega640V/ATmega1280V/ATmega1281V:
• 0 - 4MHz @ 1.8V - 5.5V, 0 - 8MHz @ 2.7V - 5.5V
– ATmega2560V/ATmega2561V:
• 0 - 2MHz @ 1.8V - 5.5V, 0 - 8MHz @ 2.7V - 5.5V
– ATmega640/ATmega1280/ATmega1281:
• 0 - 8MHz @ 2.7V - 5.5V, 0 - 16MHz @ 4.5V - 5.5V
– ATmega2560/ATmega2561:
• 0 - 16MHz @ 4.5V - 5.5V

Table 3: Technical Overview of the memory used for the Relay/XOR unit

Cypress 62128	
■Very high speed: 45 ns ■ Voltage range: 4.5 V to 5.5 V ■ Pin compatible with CY62128B	■ Temperature ranges ❒ Industrial: –40 °C to +85 °C ❒ Automotive-A: –40 °C to +85 °C ❒ Automotive-E: –40 °C to +125 °C

■ Ultra low standby power	■ Ultra low active power
❒ Typical standby current: 1 ▢A	❒ Typical active current: 1.3 mA at f = 1 MHz
❒ Maximum standby current: 4 ▢A (Industrial)	■ Easy memory expansion with CE1, CE2, and OE features
■ Automatic power down when deselected ■ Complementary metal oxide CMOS for optimum speed / power	■ Offered in standard Pb-free 32-pin STSOP, 32-pin SOIC, and 32-pin thin small outline package (TSOP) Type I packages

Table 4. Technical Overview of the communication interface used for the XOR unit

Wiznet W5500	
- Supports Hardwired TCP/IP Protocols : TCP, UDP, ICMP, IPv4, ARP, IGMP, PPPoE - Supports 8 independent sockets simultaneously - Supports Power down mode - Supports Wake on LAN over UDP - Supports High Speed Serial Peripheral Interface(SPI MODE 0, 3) - Internal 32Kbytes Memory for TX/RX Buffers	- 10BaseT/100BaseTX Ethernet PHY embedded - Supports Auto Negotiation (Full and half duplex, 10 and 100-based) - Not supports IP Fragmentation - 3.3V operation with 5V I/O signal tolerance - LED outputs (Full/Half duplex, Link, Speed, Active) - 48 Pin LQFP Lead-Free Package (7x7mm, 0.5mm pitch)

Figure 3: Energy meter type at node A plus radio unit

Referring to the equipment used for interconnecting the end devices and the aggregator units, the testbed uses a set of one **energy meter** and one **communication unit**. The energy meter is connected to the supply of each load, in Parallel to the power supply and in series to the power cord. The voltage measurement circuit gives the active potential value (Vrms). The current measurement circuit gives us the active value (Irms). The phase difference of the two vector sizes results in the power factor (cosΘ), the active power and the apparent power.

Figure 4: Energy meter at nodes B and C plus radio unit

The measurement circuit forwards all the individual measurements to the communication unit that stores, preprocesses and performs all other necessary procedures for communication with the Aggregator unit. The operation of the system includes recording the electrical quantities of the operation of each load and sending them to the central computer. We have been implemented two types of metering units. The load-disconnecting meter and the three-phase monitoring at the measurement node A (Fig. 3) as well as the simple meter that only gives us energy measurements without load interruptions (nodes B and C) – (Fig. 4).

To effectively switch on/off the units of interest of the experimental assessment scenarios, we have attached to the energy meter of the air condition (node A) and the laptop units (node B) a solid state relay (SSR) that allows distant control and switch on/off of the devices attached to it. The SSR used to implement the respective operation in the testbed was a Sharp S216S02 Series (see Table 5).

Table 5: Technical Overview of the micro-controller used for the Relay/XOR unit

Sharp S116S02 Series / S216S02 Series	
■ **Features**	■ **Agency approvals/Compliance**
1. Output current, IT(rms)≤16.0A	1. Isolated interface between high voltage AC devices and lower voltage DC control circuitry.
2. Zero crossing functionary (VOX : MAX. 35V)	2. Switching motors, fans, heaters, solenoids, and valves.
3. 4 pin SIP package	3. Power control in applications such as lighting and temperature control equipment.
4. High repetitive peak off-state voltage (VDRM : 600V, **S216S02 Series**) (VDRM : 400V, **S116S02 Series**)	
5. High isolation voltage between input and output (Viso(rms) : 4.0kV)	
6. Lead-free terminal components are also available (see Model Line-up section in this datasheet)	
7. Screw hole for heat sink	

Figure 5: Set up for Node A (air condition unit)

Moving to the **end devices**, we have selected 3 different type of loads. Firstly, the energy meter A (together with the radio unit and the SSR) are attached to an air condition unit to assess the performance using heavy loads. Secondly, the energy meter B (together with the radio unit and the SSR) are attached to a Dell Inspiron 15-5558 laptop with some additional external peripherals (sound speakers). This set of end devices has been selected to assess the performance of the protocol stack under loads that can be re-scheduled and postponed.

Thirdly, we have attached to the energy meter C (together with the radio unit) two different types of typical enterprise devices: a thermal printer (PROLINE T80) and a projector (Hitachi CP-X260 series), aiming to investigate the performance with some high priority loads.

Figure 6: Set up for Node B (laptop and speakers)

Figure 7: Set up for Node C (projector and thermal printer)

In the baseline operation of the WP-5 testbed, the communications between a) the aggregator and the central unit, b) the aggregator and the XOR unit, c) the XOR unit and the energy meters A,B and C, are performed through an Ethernet link. On the other hand, the communications between the aggregator and the energy meters A,B and C are performed through the 3G network. For the validation of the relay-based NC protocol and the measurement of the respective performance gains, the testbed has replaced the 3G links with standard Ethernet links of 10m each, aiming to easily introduce artificial path losses and test the testbed performance under challenging propagation environments. The main reason was the fact that it was extremely difficult to introduce and handle external path losses (i.e. measure the performance gain in terms of bit error rate –BER- for a given path loss increase). An overview of the baseline version of the testbed is given in Fig. 8.

Figure 8: Testbed overview

In the left of Fig. 8, we can see the central unit that is attached to the Aggregator unit with an Ethernet connection (white cable to Skylog unit). Starting with a red Ethernet cable from the Aggregator unit (located in front of the monitor) the Aggregator unit is attached to the XOR unit that is located in front of the laptop unit. The RL/XOR unit connects with the three energy meters through both 3G and Ethernet connections (red cables) over the Skylog adapter. Accordingly, Node B (middle of the table with the laptop and speakers) is attached to the RL unit through another Skylog adapter and has attached to it the energy meter of type B and the SSR for switching on/off its power. Node C is located in the right of the table, where the projector can be seen, which is also attached to the AG unit through a Skylog adapter. The energy meter of type B and the SSR can also been seen in front of the projector unit. Finally, Node A is attached to the Skylog adapter shown in the bottom right of Fig. 8.

NC Protocol

In line with the integration phase in the joint simulation setup of D5.1, the testbed implements a relay-aided communications grid where primary transmissions from the energy meters (source) to the aggregator (destination) are aided by secondary transmissions from intermediate relays/XOR units (or regular energy meters). The aim of this relay-aided network coding setup is to demonstrate the gains attained in terms of the packet error rate in the primary transmission (i.e. the receiver of the aggregator). testbed considers XOR based inter-session NC to make use of a single uplink relay instead of one per energy meter. A simplified version of the operation supported by the testbed in the network coding sub-layer is given in Fig. 9. The relay conveys the packet from energy meters "A" and "B" by performing a bitwise XOR operation, but also each packet is sent individually from each node. Even though this adds redundancy due the additional packet sent from relay R to the aggregator (here is the base station - BS), it also enables the aggregator to recover a packet loss either from A, or from B by exploiting the NC-based packet sent by the relay node R.
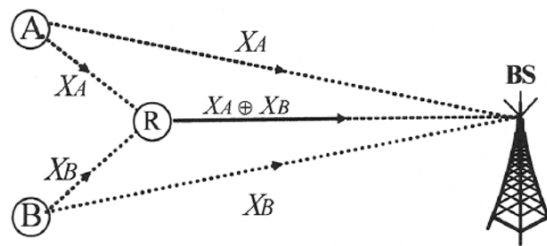

Figure 9: NC in relay-based topologies

In our testbed, the three energy meters, denoted as A, B and C here, construct packets and send them with a direct link to the aggregator unit (e.g. a 3G connection). At the same time, the relay/XOR unit (which could also be another EM) awaits for the reception of all three packets from A, B and C given a specific sequence of EM IDs per node and performs a bitwise XOR operation over the received data. Accordingly, it forwards the result of the XOR convolution to the aggregator unit using a direct link. On the one hand, we have integrated regular 3G/GSM radio units at the EMs and the AG units. On the other hand, aiming to simplify the introduction of higher channel losses and enable a simple over-hearing of the A, B and C transmissions by the relay node, we have chosen to implement the relay-aided bitwise-XOR NC scheme using Ethernet links between all units.

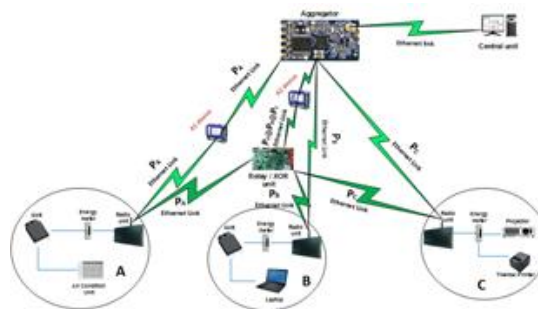**Experimental Results**

Figure 10: Schematic Diagram of the Testbed for the communication enhancements

To measure the performance gains following from the deployment of the reliable communication protocols integrated into the testbed, we have set up the testbed shown in Fig. 10 (addition of A1 and A2 analyzer devices). All 3G links between the energy meters and the aggregator unit have been replaced by Ethernet links (utilizing one additional port from the Skylog radio unit) to easily introduce path loss errors through an external attenuation device. Moving one step further, we have introduced two Datacom E-4300A metering units (analyzers) between the following two links: a) between the energy meter A and the AG unit and b) between the RL and the AG units, to introduce external path losses that can readily provide insights on the potential gains of employing the testbed reliable communication protocols. Since the resulting BER at the AG unit will strongly depend on the external path losses introduced by the analyzer units and the respective link lengths, we have evaluated the performance gains of the simplified NC protocol for different combinations of path losses and link lengths (Ethernet capable length). In the following subsections, we present the metrics used and the results for the different scenarios under scope.

Performance Evaluation Metrics

In the next subsections we use two different metrics to better highlight the performance evaluation gains following from the employment of the proposed solutions. Let $BER_{baseline}$ denote the BER without the employment of NC protocol and let the respective BER under the employment of the NC protocol to be denoted by BER_{NC}. Then, we proceed with the following two definitions:

Definition 1. The *absolute BER gain* is defined as the absolute difference between i) the BER measured under the employment of the proposed NC protocol and ii) the BER measured without the employment of the respective solutions as follows:

$$BER_G = BER_{baseline} - BER_{NC} \tag{1}$$

Definition 2. The *relative BER gain* is defined as the ratio difference between i) the BER measured under the employment of the NC protocol and ii) the BER measured without the employment of the respective solutions as follows:

$$BER_G = BER_{baseline} / BER_{NC} \tag{2}$$

At this point, we note that the need for using both metrics (absolute and relative BER gain) follows from the fact that the BER is typically given in logarithmic scale and thus, although the absolute BER gain gives a good view of the deterioration experienced without the use of the NC protocol it cannot provide useful insights on the scale of the potential gains following from the employment of the NC protocol for small differences in the link length (as seen in the next subsections.
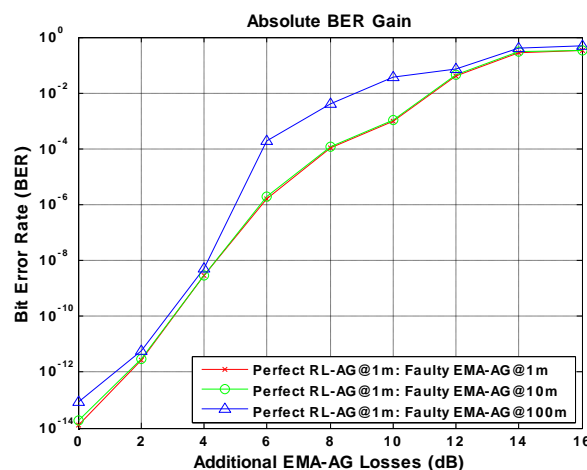
Perfect RL/AG links / Faulty AG-EM link

Figure 11: Absolute BER Gain for Perfect RL-AG link and faulty EMA-AG links – Log Scale

(Different link lengths and additional losses)

In this set of experiments we assume that the link between the RL and the AG units does not experience any external losses from the A2 device (Fig. 10). In contrast, we have considered variable attenuation (controlled by

the A1 device shown in Fig. 10) in the link between the energy meter A and the AG unit. The plots below have been derived for different combinations of the link lengths between a) the EM A and the AG unit (i.e. 1, 10 and 100m) and b) the RL and the AG unit. All plots depict the absolute difference between the BER measured at the AG unit with and without the use of the reliable communication protocols of testbed. Note that in the absence of additional path losses the BER without in the testbed was measured and given by 10^{-14}.
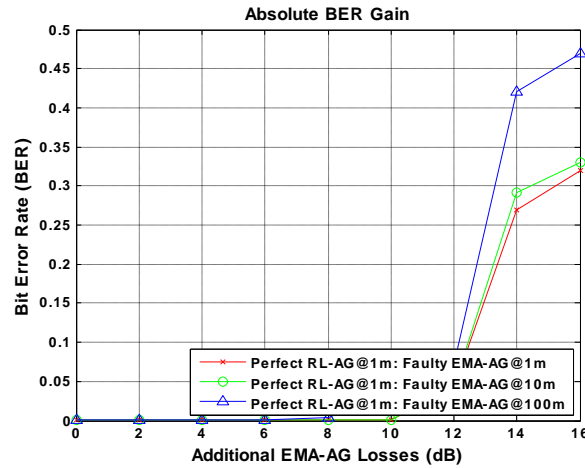

Figure 12: Absolute BER Gain for Perfect RL-AG link and faulty EMA-AG links – Linear Scale
(Different link lengths and additional losses)

In Fig. 11, we provide the absolute BER gain for three different link lengths between the energy meter A (EMA) and the aggregator unit (AG), i.e. 1m, 10m and 100m. As shown in Fig. 11, the introduction of 2 dB losses in the link between the energy meter A and the AG unit results in a roughly hundred-fold gain in terms of BER. Notably, when the link between the EMA and the AG units is larger (e.g. 100m) the respective gain is even more evident for medium to high losses (i.e. 4 to 10 dB) in the respective link. On the other hand, in terms of absolute BER gain, a one-scale increase of the link length gives roughly the same BER gain for the same value of additional EMA-AG losses. In the following plot, we provide the same results in a linear scale to reveal that severity of the path losses over 10dB and the respective BER gain following from the employment of the simplified NC solution (Fig. 12). Note that although this diagram demonstrates the important gains attained under the employment of the NC solution even under scenarios with very high interference/ path losses (i.e. above 10dB), it provides little practical information on the intervals used for real-life communications (i.e. close to 10^{-8} and below). At this point, it can be said that even the employment of the proposed simplified NC protocol for reliable communications can provide significant gains in terms of absolute BER as compared to a baseline operation of a typical Smart Grid network.

Moving one step further with our real-life experimental evaluation, we have introduced losses in the RL-AG link using the A2 device. In this set of experiments, we aim to emulate the even more challenging scenario where all links in the near proximity of the AG unit are subject to high interference, or external path losses. Provided that the link length of the RL-AG units will be equal or lower than that of the remaining direct link (i.e. EMA-AG, EMB-AG and EMC-AG), we have only evaluated scenarios where the link length of the RL-AG unit is equal or lower than that between the EMA-AG unit. To further derive valuable insights on the potential gains following from the employment of the simplified protocol for reliable communications, we have proceeded with our evaluation under equal attenuation between the EMA-AG and the RL-AG units as well as with different attenuation (additional losses) between the respective links. The results of the equal attenuation/different link length scenario are useful when the reason behind the link deterioration is within proximity of the AG unit (thus all links towards it are affected), whereas the scenario with the different attenuation and equal link lengths are more practical when the reason of the attenuation is more evident in the direct (rather than the relay) links.
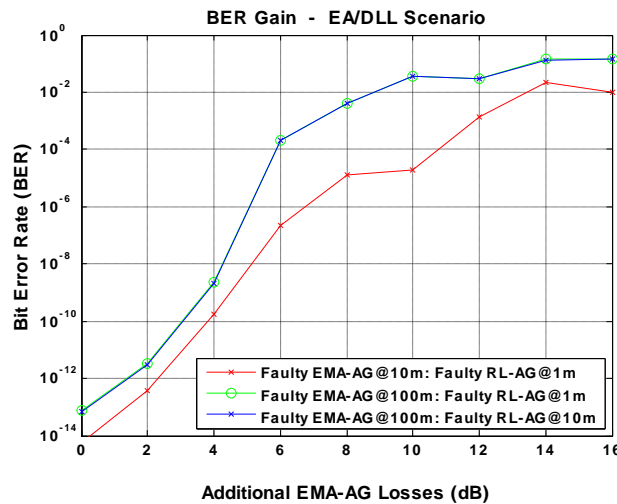
Faulty RL/AG links / Faulty AG-EM link

Figure 13: Absolute BER Gain for Faulty RL-AG link and faulty EMA-AG links under equal attenuation and different link lengths between the RL-AG and the EMA-AG units

Equal Attenuation / Different Link Length Scenario

In this scenario, we have measured the absolute BER gain when all links in the near proximity of the AG unit are subject of low SNR conditions (e.g. interference, noise or path losses). Since the RL unit should be in a distance that is at least equal or closer to the direct link, we have evaluated three different sets of link length combinations between the EMA-EGA and the RL-AG units by fixing the additional EMA-AG losses. Note that the losses in the RL-AG in the next plot have been fixed to match the ones of the EMA-AG link. As a first result, we observe that for a long distance in the direct link between the EMA and the AG unit, the distance of the RL-AG unit has a minimal impact on the BER gain attained by the NC protocol (i.e. the green and blue lines are roughly the same).

On the other hand, when the link length between the EMA-AG and the RL-AG links are comparable (i.e. red line) the respective BER gain is notable but lower as compared to that where the direct link is comparably higher than the relay link (i.e. when EMA-AG is set at 100m). In both cases, the BER gain attained by the employment of the NC solutions can play a critical role in the reliability of smart grid communications, since for example when a minimum BER threshold of 10^{-8} is required, the employment of the NC protocols can alleviate channel errors following from the presence of losses that can reach up to 6 dB (i.e. 4 times lower SNR).
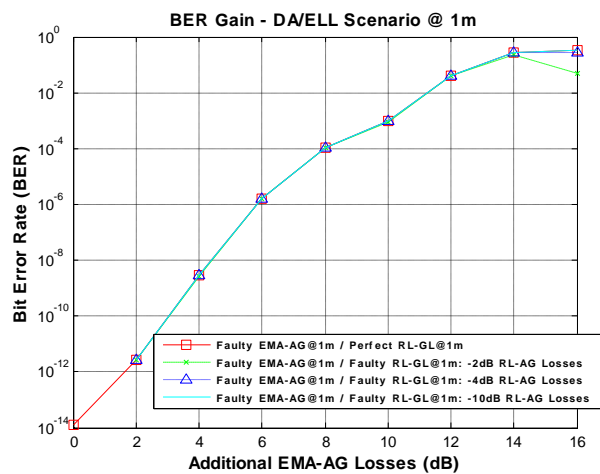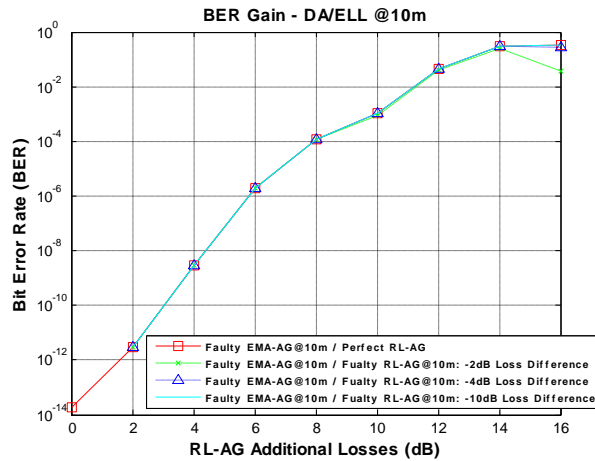

Figure 14: Absolute BER Gain for Faulty RL-AG link and faulty EMA-AG links under equal attenuation and link length equal to 1m for the RL-AG and the EMA-AG links

Different Attenuation / Equal Link Length

Figure 15: Absolute BER Gain for Faulty RL-AG link and faulty EMA-AG links under equal attenuation and link length equal to 10m for the RL-AG and the EMA-AG links

In Fig. 16 we plot the absolute BER gain following from the employment of the NC protocol for increasing losses in the EMA-AG links. The link length between the RL-AG and the EMA-AG links have been set to be equal, whereas the RL-GL link is either assumed to be perfect (red square plot), or to experience a better propagation environment with 2dB (green x plot), 4dB (dotted blue triangle plot), or 10dB (cyan plot) higher SNR compared to the EMA-AG link (or 2dB, 4dB and 10dB lower losses). In absolute values, the BER gain following from the employment of the NC solution remains roughly unaffected with respect to the link gains introduced in the RL-GL link. The gain grows roughly a hundred-fold for every 2dB additional loss in the EMA-AG channel. Comparable BER performance has been recorded for longer link distances (i.e. for 10m and 100m link) between the RL-AG and the EMA-AG units as shown in Fig. 17-18, indicating that for an equal link length yet different channel conditions between the RL-AG and the EMA-AG units the gain remains roughly unaffected.
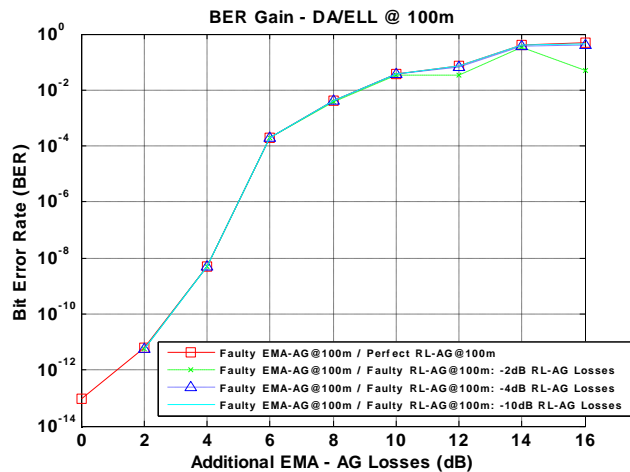

Figure 16: Absolute BER Gain for Faulty RL-AG link and faulty EMA-AG links under equal attenuation and link length equal to 100m for the RL-AG and the EMA-AG links

At this point, it is important to note that even though the absolute BER difference with and without the employment of the NC protocol is roughly the same for different link lengths, this effect has primarily to do with the fact that the enhanced BER performance dominates in the subtraction of the BER metrics the one without the employment of the NC protocol.
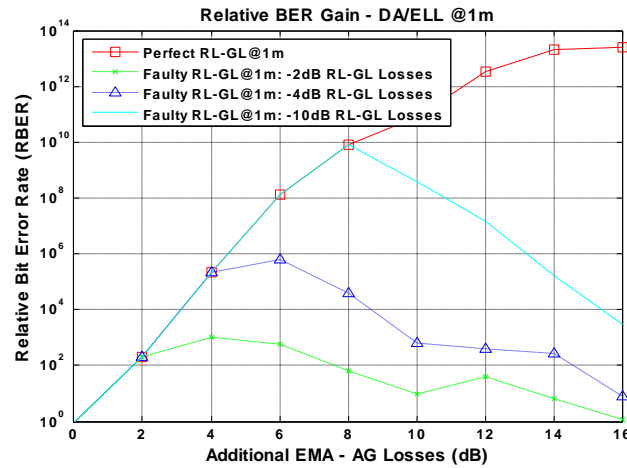
Figure 17: Relative BER Gain for Faulty RL-AG link and faulty EMA-AG links under equal attenuation and link length equal to 1m for the RL-AG and the EMA-AG links

To this end, in Figs. 18-19 we depict the relative BER gain following from the employment of the NC protocol aiming to identify and better highlight the conditions under which the performance gains are maximized as compared to the baseline scenario (no NC protocols). Interestingly, as shown in Fig. 19, in a relative scale the NC protocols exhibit an optimal point to which the NC solution provides the optimal performance improvement when the RL-AG and the EMA-AG units experience different channel conditions. Notably, in an absolute scale this point couldn't be identified since the subtraction of the BER and the baseline BER was dominated by the first term (BER). As shown in Fig. 18, different optimal operation points are identified for different RL-AG attenuations under the same RL-AG / EMA-AG link lengths. When the RL-GL experiences 2dB better channel conditions as compared to the one experienced in the EMA-AG link, the maximum gains are attained when the EMA − AG loss is close to 4dB. On the other hand, when the RL-GL experiences 4dB better channel conditions as compared to the one experienced in the EMA-AG link, the respective maximum gain point is observed for 6dB losses in the EMA-AG link, whereas for 10dB better channel conditions the respective maximum relative gain is observed for 8dB EMA-AG losses. This result, not only reveals the multifold increase of the BER supported by the NC protocol, but also establishes the existence of a maximum performance gain in the relative scale.
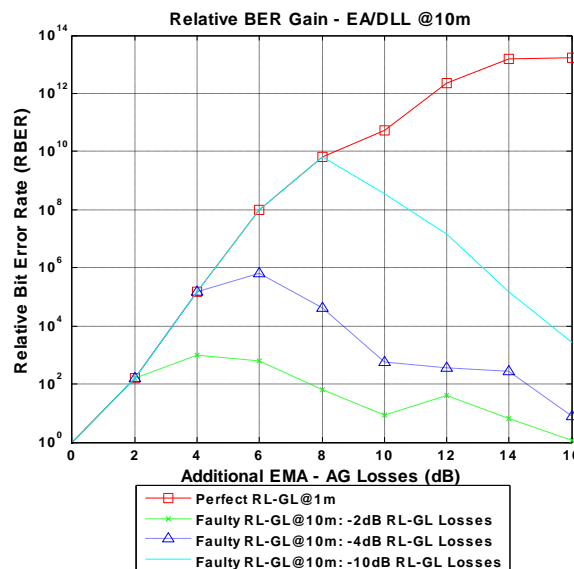

Figure 18: Relative BER Gain for Faulty RL-AG link and faulty EMA-AG links under equal attenuation and link length equal to 10m for the RL-AG and the EMA-AG links
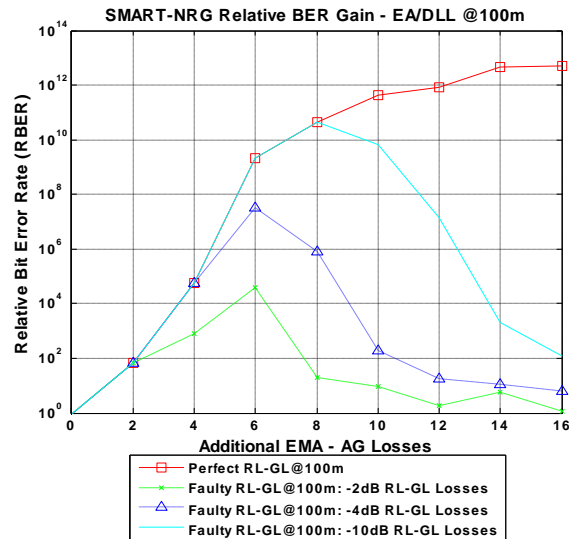
Figure 19: Relative BER Gain for Faulty RL-AG link and faulty EMA-AG links under equal attenuation and link length equal to 100m for the RL-AG and the EMA-AG links

In Fig.19, we plot the corresponding results when the link length between the RL-AG and the EMA-AG units is equal to 10m. Similar to Fig. 18, the maximum relative gain is observed very close to that observed for the 1m link length. However, as shown in Fig. 19, the relay-based NC communication protocol can support even higher relative gains when the link length is comparably higher (i.e. close to 100m).

Conclusion

In this paper we have used an experimental testbed to demonstrate the benefits following from the employment of a simplified protocol for relay-based network coding communications in the smart grid. Our experimental results show that the employment of even a simplified version of such a reliable communication protocol can greatly improve network performance in the Smart Grid. In our future work, we aim to experimentally assess the performance of more sophisticated network coding protocols and optimize their operation in the context of the Smart Grid.

References

[1]. C. H. Hauser et al., "A failure to communicate: Next-generation communications requirements, technologies, and architectures for the electric power grid", IEEE Power and Energy Mag., Apr. 2005.

[2]. V. C. Gungor et al., "Smart grid technologies: Communication technologies and standards", IEEE Trans. Industrial Informatics, Nov. 2011.

[3]. N. Kayastha et al., "Smart grid sensor data collection, communication, and networking: A tutorial", Wireless Commun. Mobile Comput., John Wiley & Sons, July 2012.

[4]. Fang, Xi; Misra, Satyajayant; Xue, Guoliang; Yang, Dejun, "Smart Grid — The New and Improved Power Grid: A Survey," Communications Surveys & Tutorials, IEEE , vol.14, no.4, pp.944,980, Fourth Quarter 2012.

[5]. European communications, "M2M beyond connectivity", Q3 2012 issue.

[6]. V.C. Gungor, D. Sahin, T. Kocak, S. Ergut, C. Buccella, C. Cecati, G.P. Hancke, "Smart Grid Technologies: Communication Technologies and Standards", IEEE Transactions on Industrial Informatics, vol.7, no.4, pp.529-539, Nov. 2011.

[7]. Ahlswede et. al. "Network Information Flow". IEEE Transactions on Information Theory 2000

[8]. P. Elias, A. Feinstein, and C. E. Shannon, "Note on maximum flow through a network," IRE Transactions on Information Theory IT-2, pp. 117–199, 1956

[9]. P. Pahlevani, M. Hundebøll, M.V. Pedersen, D. E. Lucani, H. Charaf, F. H.P. Fitzek, H. Bagheri, M. Katz, "Novel Concepts for Device to Device Communication using Network Coding," accepted to IEEE Communications Magazine (in press), 2014

[10]. A.G. Dimakis, K. Ramchandran, Y. Wu, C. Suh, "A Survey on Network Codes for Distributed Storage," Proceedings of the IEEE, Vol. 99, No. 3, March 2011.

[11]. Tsiota, D. Xenakis, N. Passas, L. Merakos, "Jamming and Black Hole Attacks in the Smart Grid with Perfect Detection of Malicious Nodes", IEICE ICTF, Patras – Greece, June 2016.

[12]. D. Xenakis, M. Kountouris, L. Merakos, N. Passas, and C. Verikoukis, "Performance Analysis of Network-Assisted D2D Discovery in Random Spatial Networks", IEEE Transactions on Wireless Communications, Vol. 15, Iss. 8, Aug. 2016.

Nikos Passas received his Diploma (honors) from the Department of Computer Engineering, University of Patras, Greece, and his Ph.D. degree from the Department of Informatics and Telecommunications, University of Athens, Greece, in 1992 and 1997, respectively. Since 1995, he has been with the Communication Networks Laboratory of the University of Athens, working as a lecturer and senior researcher in a number of national and European research projects. He has also served as a guest editor and technical program committee member in prestigious magazines and conferences, such as IEEE Wireless Communications Magazine, IEEE VTC, IEEE PIMRC, IEEE Globecom, etc. Dr. Passas has published more than 100 papers in peer-reviewed journals and international conferences and has also published 1 book and 10 book chapters. His research interests are in the area of mobile network architectures and protocols.